INVESTIGATIONS ON THE X-RAY STRUCTURAL STUDIES AND DOCKING ANALYSIS OF 1–(4–CHLOROPHENYL) – 3 PHENYL – 3 – (4,5,6,7 –TETRAHYDROBENZO [D] [123]SELENADIAZOL 4 –YL) PROPAN –1–ONE

[1]Dr. A. V. Jhone Verjhula, [2]Ms. Gracie. P.J, [3]Dr. A. Jeyabharathi
[1]Head of the Department, [2]Assistant Professor, [3]Former Professor
Department of Physics
Ethiraj College for Women (Autonomous), Chennai, Tamil Nadu, India

Abstract: The small molecule of selenadiazole in the fused pyrazole moeity is found to exhibit anti-angiogenic activity inhibiting tumour cell colony formation. This study investigates the conformation, packing, molecular geometry and structural analysis of selenadiazole derivative of a pyrazole ring with the formula C_{21} H_{20} Cl N_2 O Se. Further this compound was used for computational molecular docking analysis with the heat shock protein which is a significant anti-cancer drug target. The binding sites were predicted through molecular modeling. The derivatives of selenadiazole are seemingly potential anti-tumor drug targets.

1. I. Introduction

Characterized by a five membered ring structure composed of three carbon atoms and two nitrogen atoms in adjacent positions, pyrazole with molecular formula $C_3H_4N_2$ belongs to heterocyclic series of aromatic ring organic compounds. Studies have shown that derivatives of pyrazole exhibit antimicrobial, anticancer, ACE inhibitory, antiviral as well as anti-inflammatory effects.[1] Compounds with the fused pyrazole quinololine motifs are anti-angiogenic compounds, capable to inhibit the growth of human breast (MCF-7) and cervical (Hela) carcinoma cells *in vitro*.[1] The small molecule of selenadiazole in the fused pyrazole ring (Fig.1) is an organoselenium compound with a broad spectrum of anti-tumour activity. When a series of substituted selenadiazoles were tested for their *in vitro* anti-proliferative and cytotoxic activities against leukemia (CCRF-CEM), colon (HT-29), lung (HTB-54) and breast (MCF-7) cancer cells, they were found to exhibit remarkable activity against MCF-7 cells.[2] 1,2,3-selenadiazole substituted compounds showed promising antifungal, antibacterial, and *in vitro* antitumor activities as well.[3]

In the present study, after the X-ray structural analysis of the title compound, it was used for computational docking analysis with the heat shock protein (HSP90) coded 2CCT as shown in Fig. 2. Further, studies show that heat shock protein (HSP90), adenosine triphosphate (ATP)-dependent molecular chaperone, is a potential anti-cancer drug target. It has several oncogenic client proteins involved in signal transduction, cell cycle regulation and apoptosis.[4] HSP90 and p23 protein levels are found to be highly expressed in breast cancer cell lines.[5] Blocking nuclear HSP90 function in advanced breast cancers may be a more targeted approach for treating advanced breast cancers that are refractory to traditional therapy.[5] HSP90 activity inhibition may be used for the selective radiosensitization of the vascular endothelium involved in tumor-stimulated angiogenesis.[6] HSP90 expression in malignant cells is reported to be constitutive, and is 2 to 10 fold higher than in normal cells, indicating its vital role in the survival and growth of cancer cells, and can thus serve as an effective drug target.[7] Inhibition of HSP90 in tumor cells results in dissociation from client proteins, induces apoptosis, and reduces chemotherapy resistance in aggressive cancers.[8,9]

Synthetic selenadiazole derivatives inhibit the proliferation, invasion and migration of MCF-7 cells, promoted by hyperglycemia.[10] 2-(phenylamino)-selenazole[5,4-b]-pyridine showed higher growth inhibition and proapoptotic activity in MCF-7 human breast carcinoma cells.[11]

2. II. Experimental

Good quality single crystals of the title compound obtained from the slow evaporation method, were chosen for X-ray diffraction analysis.

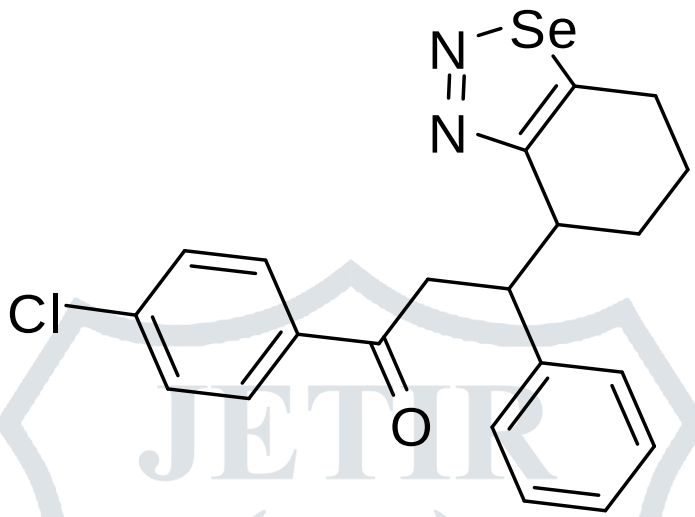

Fig. 1 Molecular Structure of
1–(4–chlorophenyl) – 3 phenyl – 3 – (4,5,6,7 –tetrahydrobenzo [d] [123] selenadiazol 4 –yl) propan –1–one

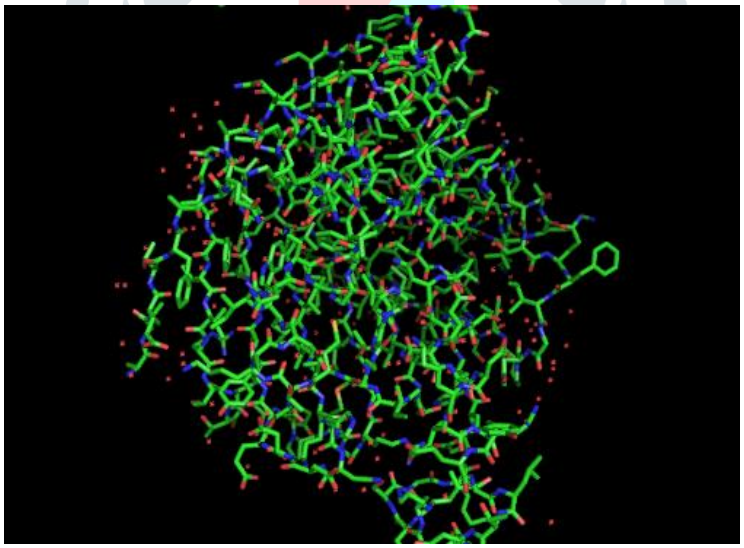

Fig. 2 Heat Shock Protein 90 (2CCT)

The measured Bragg intensities were collected using Eos CCD detector (Oxford Diffraction, 2009). The crystal of suitable dimension was mounted and accurate values of the unit cell parameters were obtained by least square analysis of high Bragg angle reflections. The Bragg reflections were measured with MoK$_\alpha$ radiation. Intensity data was collected at 293 K. All the intensities were corrected for variable scan speed, background and attenuation. The following programs were used for the structure solution, structure refinement and structure analysis: SHELXS 97[12]; SHELXL 97[13]; PLATON[14,15]; ORTEP[16].

Molecular docking studies of the given ligand, selenadiazole derivative has been done using GOLD software, a genetic algorithm for docking flexible ligands into protein binding sites, which includes the additional software components, Hermes and Goldmine.

The Hermes visualizer was used in the preparation of input files for docking with GOLD, visualization of docking results and calculation of descriptors. The Hermes visualizer was also used for interactive docking setup, for defining the binding site and setting of constraints. Table 1 shows the details of the Heat Shock Protein (HSP90)

Table 1 Details of Heat Shock Protein (HSP90)

Four letter code	2CCT
Classification	Chaperone
Molecular weight	26981.82 daltons
Molecule	Heat Shock Protein HSP – 90 ALPHA
Polymer	1
Type	Polypeptide
Chain	A
Method	X-ray Diffraction
Resolution	2.30 Å

3.

4. III. Results and discussion

The crystal structure of the title compound has been solved by SHELXS 97 and refined by SHELXL 97 program. It was found that the compound consists of a primitive, monoclinic unit cell which crystallizes in the $P2_1/c$ space group symmetry. The crystal data are presented in Table 2. ORTEP program was used to obtain the thermal ellipsoidal plot and is shown in Fig.3. The dimer formation in the compound and the packing diagram as visualized by PLATON is shown in Fig.4.

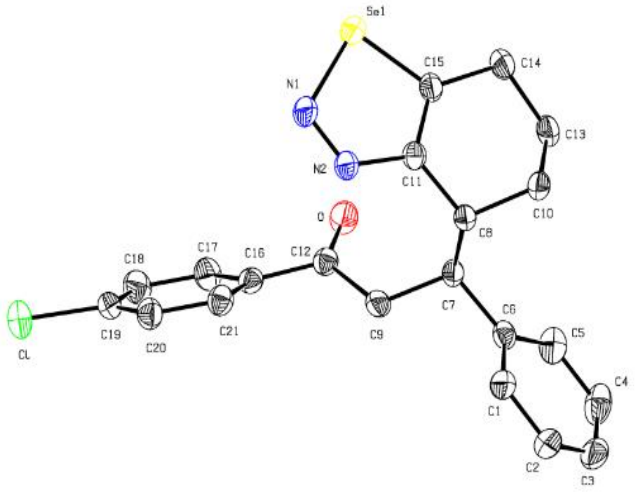

Fig. 3 Thermal ellipsoidal plot of the title compound

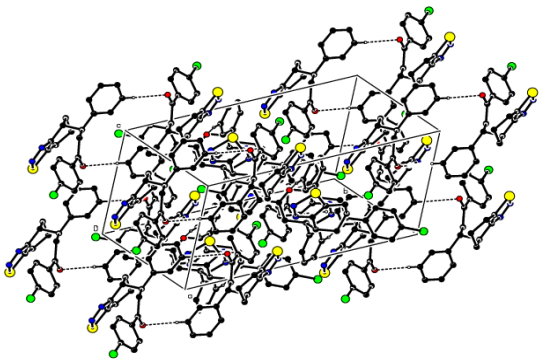

Fig. 4 Packing diagram representing dimer formation

Of the various possible conformations of a six membered ring, the six membered ring fused to the pyrazole ring is found to adopt half chair conformation[17] with the puckering parameters for the ring $Q_2 = 0.375(3)$ Å, $Q_3 = 0.327(3)$ Å and $\varphi_2 = 85.9(5)^0$.The asymmetry parameter ΔC_2 of the pyrazole ring for the best two fold axis passing through the atom N1 and the bond C11–C15 is $0.3(3)^0$ which confirms the half chair conformation.The asymmetry parameters ΔC_2 of the fused benzene ring for the best two fold axis passing through C10–C13 and C15–C11 is $3.9(4)^0$ which confirms its half chair conformation.The chlorophenyl ring is planar while the attached chlorine atom deviates by 0.019(1)Å. The C11– N2 bond length in the pyrazole ring is 1.369(4)Å which is shorter than C–N single bond length (1.443Å), but is longer than a double bond length of 1.269Å[18,19] indicating electron delocalization.

The N1=N2 bond length of 1.272(4)Å in the Pyrazole moiety is indicative of double bond character. The C–C bond lengths of the fused benzene ring shows a single bond character, except C15=C11 due to the fusion of benzene ring with the pyrazole ring that exhibits double bond character (1.367 (4)Å). The C12–C16 bond length (1.486(4) Å) is shorter due to the stabilization of the negative charge on the oxygen atom of the keto group. The C=O bond length is 1.212(4)Å which agrees with the reported values.[20] The Se–N1 distance of 1.878(3) Å is quite long when compared to the standard value, but such a variation has already been reported.[21,22] The bond lengths in the structure are comparable with the literature values; however variations in some bonds are noted. The widening of the bond angles at C11 and C15 and the constriction of the angles at C8, C10, C13 and C14 in the benzene ring are attributed to the fusion of small pyrazole ring with benzene ring.

The pyrazole ring is co-planar to the plane of the fused benzene ring with a dihedral angle of 3.39(1)Å. The dihedral angle between the pyrazole ring and the phenyl ring planes is $38.99(1)^0$. The dihedral angle between the chlorophenyl ring and the phenyl ring planes is $57.52(1)^0$. The chlorine atom substituted at C19 is in equatorial position to the chlorophenyl ring evidenced by the torsion angles [Cl – C19 – C20 – C21 =] – $178.3(3)^0$and [Cl – C19 – C18 – C17 =] $177.9(3)^0$. The keto group attached at C16 is in equatorial orientation with respect to the chlorophenyl ring as indicated by the torsion angles [C18 – C17 – C16 – C12 =] – $176.6\ (3)^0$and [C20 – C21– C16 – C12 =] $176.1(3)^0$. The chlorophenylpropan – 1– one group at C7 is in equatorial orientation with respect to the phenyl ring as indicated by the torsion angles [C2 – C1 – C6 – C7 =] $176.0(3)^0$ and [C4 – C5 – C6 – C7 =] – $176.2(3)^0$.

The keto group at C12 is axially oriented to the fused benzene ring as indicated by the torsion angle [C8 – C7 – C9 – C12 =] $90.5(3)^0$. The interesting feature of the crystal structure is the short intermolecular C4…..O (3.393(4)Å) interaction which stabilizes the molecule and the crystal structure. In the crystal, pairs of C–H…O hydrogen bonds connect the neighbouring molecules into dimers, generating $R\ {}^{2}_{2}(16)$ motifs. The proton donor capacity of C4 – H4 group is pronounced due to sp^2 hybridization of the C4 atom. In addition to van derWaals forces, the crystal is further stabilized by the C–H…πinteraction as already been reported[19] involving C13 and H13 atoms and the centroid of the six membered phenyl ring with the corresponding symmetry codes 1– x, 1 – y and –1 – z. The hydrogen bond geometry is shown in Table 3.

Table 2 Crystal data

Parameters	**Pyrazole derivative**
Formula	C_{21} H_{20} Cl N_2 O Se
Formula Weight	430.815
Temperature	293 K
Wavelength (Mo K_α)	0.71073 Å
Crystal System, Space group	Monoclinic, P 2_1 / c
Unit cell dimensions	a = 8.983(1) Å
	b = 23.252(4) Å
	c = 9.034(3) Å
	β = 92.64(2)°
Volume	1885.0(8) $Å^3$
Z	6
Calculated density	2.2770 mg/m^3
Absorption coefficient	3.215 mm^{-1}
F(000)	1314
Crystal Size	0.4 x 0.2 x 0.1 mm
Theta range for data collection	2.9 to 29.4 deg.
Index ranges	–12 < = h < = 11
	–31 < = k < = 31
	–11 < = l < = 11
Reflections collected / unique	20251/4671 [R (int) = 0.0763]
Refinement method	Full-matrix least-squares on F^2
Data / Restraints / Parameters	4671, 0, 235
Goodness of fit on F^2	0.826
Final R indices [I > 2.0 sigma (I)]	R1 = 0.0421, wR2 =0.0968
R indices (all data)	R1 = 0.0847, wR2=0.1040
Largest diff. peak and hole	– 0.26, 0.61(e $Å^{-3}$)

Table 3 Hydrogen bond geometry

D – H…A	**D – H (Å)**	**H … A (Å)**	**D … A (Å)**	**D – H … A (°)**
C – H … O [i]	0.93	2.51	3.393 (4)	158
C – H … Cg [ii]	0.97	2.91	3.781(4)	150

Symmetry codes: (i) –x, 1 – y, – 1 – z (ii) 1 – x, 1 – y, –1 – z

The interaction of the ligand with the protein from which the active site residues and the active water molecules was found and is shown in Fig.5. The docked complex is highlighted in Fig. 6. All the images have been visualized using Pymol software. Table 4 gives the docking results for the best 4 poses with the GOLD score and the hydrogen bond interactions between the ligand and the active site residues for the respective poses.

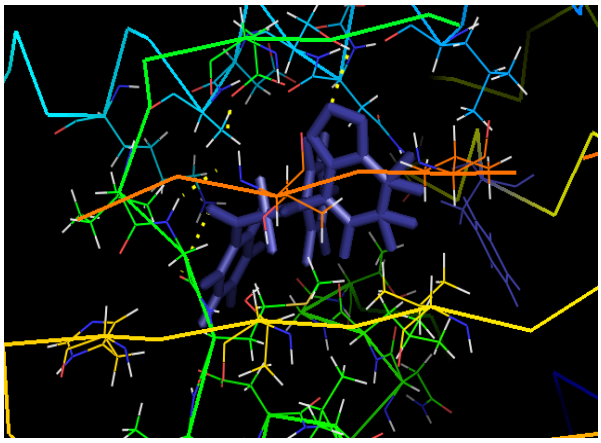

Fig. 5 Interaction of the ligand with protein

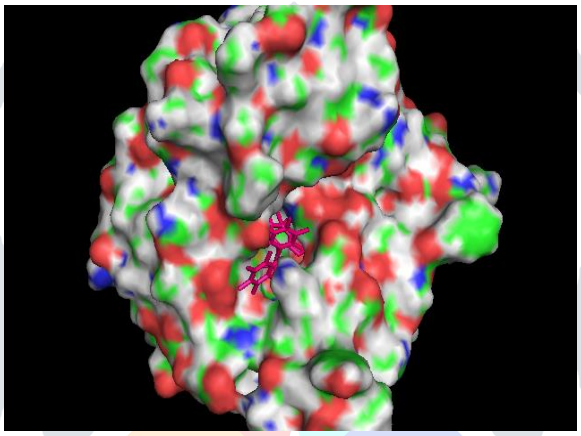

Fig. 6 Docked complex of the title compound in HSP90

The protein residues namely Asn 51, Asp 102, Ser 52 along with three stable water molecules were found to have strong interaction with the ligand from the docking analysis. The GOLD score varies from 36 to 52 while the GOLD energy ranges from –10.54k cal/mol to–11.63kcal/mol.

Table 4 Induced fit docking results

Pose	Hydrogen-Bond Interactions	Distance (Å)	Docking Score	Gold Energy kcal/mol
1.	Asn 51 (N – H…O)	2.897	52	– 10.94
2.	Ser 52 (O – H…N) Asn 51 (N – H…N)	2.816 2.585	59	– 11.63
3.	Asn 51 (N – H…O)	2.753	48	– 10.94
4.	Asp 102 (O – H…O) Asp 102 (O – H…O)	2.710 2.533	36	– 10.54

IV. Conclusion

The title compound of the selenadiazole derivative was analyzed by X- ray diffraction for its crystal structure, packing geometry and conformation. The results obtained were in agreement with the reported values of similar compounds. The binding sites in the target protein were predicted through docking analysis. Gold score obtained in the above study predicts that the ligand binds well in the active sites of the said protein with fairly good interaction with the amino acid residues. The computational docking analysis

of C_{21} H_{20} Cl N_2 O Se reveals that such compounds inhibit HSP90. Hence it is suggested that these derivatives could be taken for *in vitro* and *in vivo* studies to emerge as potential anti- tumour candidates.

References

[1] Alka Chauhan, P. K. Sharma, Nirajan Kaushik. (2011). 'Pyrazole: A Versatile Moiety'. *International Journal ChemTechResearch*. 3 (1):11 – 17.

[2] Plano, D (Plano, Daniel), Moreno, E (Moreno, Esther), Font, M (Font, Maria), Encio, I (Encio, Ignacio), Palop, JA (Antonio Palop, Juan), Sanmartin, C (Sanmartin, Carmen). (2010). Synthesis and in vitro Anticancer Activities of some Selenadiazole Derivatives. 343:680 - 691.

[3] Mhaidat N, Al-Smadi ML, Al- Momani F, Alzoubi K H, Mansi I, Al-Balas Q. (2015). Synthesis, antimicrobial and in vitro antitumor activities of a series of 1,2,3-thiadiazole and 1,2,3-selenadiazole derivatives. 2015:3645-3652.

[4] Saxena, A. K., Saxena, S. and Chaudhary, S.S. (2011). *Bio.Org. Med. Chem*, 19 (5):1714 - 20.

[5] Malissa C. Diehl, Michael O. Idowu, Katherine Kimmelshue, Timothy P. York, Lynne W. Elmore and Shawn E. Holt. (2009). Elevated expression of nuclear Hsp90 in invasive breast tumors. *Cancer Biology & Therapy*. 8:20, 1952-1961.

[6] Vladimir A. Kudryavtsev, Anna V. Khokhlova, Vera A. Mosina, Elena I. Selivanova, and Alexander E. Kabakov. (2017).Induction of Hsp70 in tumor cells treated with inhibitors of the Hsp90 activity: A predictive marker and promising target for radiosensitization. 12(3): e0173640.

[7] Ferrarini M, Heltai S, Zocchi MR, Rugarli C. (1992). Unusual expression and localization of heat-shock proteins in human tumor cells. *Int J Cancer*. 51:613 – 9.

[8] Connell P, Ballinger CA, Jiang J, et al. (2001). The co-chaperone CHIP regulates protein triage decisions mediated by heat-shock proteins. *Nat Cell Biol*. 3:93 – 6.

[9] Elah Pick, Yuval Kluger, JenniferM. Giltnane, Christopher Moeder, Robert L. Camp, DavidL. Rimm and Harriet M. Kluger. (2007).High HSP90 Expression Is Associated with Decreased Survival in Breast Cancer. *Cancer Res*. 67(7):2932-2937.

[10] Jianfu Zhao, Delong Zeng, Yuedan Liu, Yi Luo, Shengbin Ji, Xiaoling Li and Tianfeng Chen. (2017). Selenadiazole erivatives antagonize hyperglycemia-induced drug resistance in breast cancer cells by activation of AMPK pathways. *Metallomics*. 9:535-545.

[11] Desiree Bartolini, Luca Sancineto, AndrezaFabro de Bem, Kenneth D. Tew, Claudio Santi, Rafael Radi, PierangeloToquato, Francesco Galli. (2017). Selenocompounds in Cancer Therapy: An Overview. *Advances in Cancer Research*, Volume 136:273.

[12] Sheldrick, G.M. (1997b). SHELXS 97 Program for the Solution of Crystal Structure. University of Gottingen, Germany.

[13] Sheldrick, G.M. (1997c). SHELXS 97 Program for the Refinement of Crystal Structures. University of Gottingen, Germany.

[14] Spek, A. L. (2003). *J. Appl. Cryst*. 36: 7-13.

[15] Spek, A. L. (2009). *Acta Cryst* . D 65: 148 – 155.

[16] L.J. Farrugia. (1997). Ortep3 for Windows, *J. Applied. Cryst*., 30, 565.

[17] J. Muthukumaran, M. Nachiappan, S. Chitra, P. Manisankar, SumanBhattacharya, S. Muthusubramanian, R. Krishna, and J. Jeyakanthan. (2011). 1-(2-Naphthyl)-3-phenyl-3-(4,5,6,7-tetrahydro-1,2,3-

benzoselenadiazol-4-yl)propan-1-one. ActaCrystallogr Sect E Struct Rep Online. 67(Pt 8): o2010–o2011.
[18] Jin, Z.-M., Li, L., Li, M.-C., Hu, M.-L. and Shen, L.(2004). *ActaCryst*.,C 60:o 642 - o643.
[19] V. Susindran, S. Athimoolam, S. Asath Bahadur, R. Manikannan and S. Muthusubramanian. (2010). (E)-3-
(4-Chlorophenyl)-3-[3-(4-chloro-phenyl)-1H-pyrazol-1-yl]prop-2-enal.ActaCryst.E66:o2594-o2595.
[20] Hai Yue, Wei-Li Dong, Run-Ling Wang and Xian-Chao Cheng. (2010). *ActaCryst.* E66: o 2961.
[21] Allen, F.H., Kernard, O., Watson, D.G.,Brammer, L. Orpen, A.G. and Taylor,R. (1987). *J.Chem.Soc.,Perkin*
Trans.II, S1-S19.
[22] Guillermo, A. Morales and Frank, R. Fronczek. (1994). The Crystal Structure of a
cyclodecabis[1,2,3]selenadiazole. Journal of Chemical Crystallography. 24 (12): 811- 813.